Polarimetry and Star Formation in the Submillimeter

Brenda C. Matthews

Radio Astronomy Laboratory, Department of Astronomy, University of California, 601 Campbell Hall, Berkeley, CA, 94720, U.S.A.

Abstract.
Polarimetry in the submillimeter is the most effective probe of magnetic fields in star-forming regions. Linearly polarized emission is detected from dust on all scales and at all wavelengths observed in molecular clouds. Linear polarization of CO has been detected in several outflows and even in the envelope of a high mass core. This method gives access to the field geometry in environments inaccessible via dust polarimetry. I discuss primarily the results from the SCUBA and Hertz polarimeters and the BIMA array. I also discuss the spectroscopic technique of estimation of the magnetic field inclination to the line of sight by comparison of ionic and neutral field lines. Without requiring a polarimeter, this method has the potential of greatly expanding the impact of polarimetric data. Finally, I summarize the potential of future polarimeters to further expand our understanding of the role of the magnetic field in star formation and molecular cloud processes.

1. Introduction

Star formation is fundamentally a multi-scale problem. The process involves physics from the scales of molecular clouds to cores, disks and protostars, a difference of several orders of magnitude in scale and 10^6 in mass. A fundamental problem in the study of star formation is the determination of what mechanism prevents clouds from collapsing on large scales and regulates star formation to the low efficiency we observe. It has long been known that the thermal support within clouds is insufficient to provide support to more than a few solar masses of gas. Whether or not all regions of molecular clouds could collapse to form stars (Elmegreen 2000), or all cores can become star-forming (Vázquez-Semadeni, Ballesteros-Paredes & Klessen 2003), some additional force must be present on large scales to provide support. Static magnetic fields or MHD waves are the two most likely sources. Even in light of recent arguments that star formation may be so rapid that ambipolar diffusion may not be required in cores (Hartmann, Ballesteros-Paredes & Bergin 2001), measurements suggest that magnetic fields are present.

The observational evidence for magnetic fields and turbulence is well known. Within dense cores, Zeeman splitting of OH, CN and CCS molecules reveal magnetic fields present at levels of tens of microgauss to several milligauss (i.e., Bourke et al. 2001; Levin et al. 2001; Crutcher et al. 1999). Evidence for turbulent motions in clouds is also well established, since measured linewidths are much wider than thermal values, with the most non-thermal contributions arising in the most massive clouds (Larson 1981).

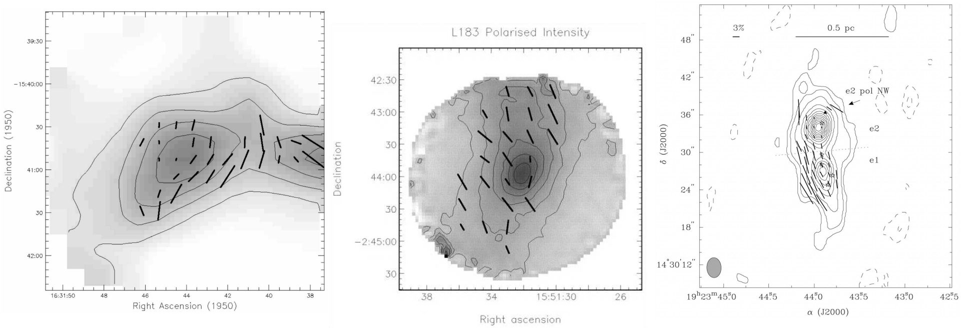

Figure 1. Polarization maps of pre-stellar and high-mass cores. The two pre-stellar cores, L43 (left, Crutcher et al. 2004) and L183 (center, Ward-Thompson et al. 2000), show evidence of variations in vector orientation despite an overall trend of alignment along the minor axis. Vectors shown are rotated 90° from the polarization direction to yield a net magnetic field direction according to grain alignment theory. The polarization map of the high mass region W51 at right was obtained with the BIMA array (Lai et al. 2001). W51 contains two cores, e1 and e2, with aligned polarization vectors along the ridge between them. In each region, the polarization percentage drops toward regions of higher flux. These polarization holes are typical of most polarization maps.

Measurement of the magnetic field geometry within molecular clouds is best done using polarized emission from dust at far-infrared to millimeter wavelengths (Hildebrand 1988). At long wavelengths ($\lambda > 60$ μm), dust grains aligned by a magnetic field produce polarized emission orthogonal to the field direction. While no estimate of the field strength is possible, the vector orientation yields the projected field geometry on the plane of the sky (see Figure 1), or at least a vector sum of the projected field through the cloud which can be compared with models. While Zeeman splitting has proven difficult to detect (Crutcher 1999), polarized emission from dust is detectable over a range core masses and spatial scales with the recent improvements in bolometer sensitivity at submillimeter and millimeter wavelengths. In fact, the success of polarimetry with the SCUBA (Submillimetre Common User Bolometer Array) and Hertz polarimeters on the James Clerk Maxwell Telescope (JCMT) and Caltech Submillimeter Observatory (CSO) suggests that sensitivity is the only limitation to detection of polarized emission from dust throughout molecular clouds.

2. Instrumentation

The earliest dust emission polarimetry was done in the far-infrared at 100 and 270 μm by the Kuiper Airborne Observatory (KAO) over the period of 1984 to 1998. Dotson et al. (2000) presents a consistent re-reduction of all the KAO 100 μm polarimetry data. Polarimetry of dust is practical to wavelengths of $\sim$ 1 mm; at longer wavelengths, free-free emission begins to make signficant contributions to the continuum, while the dust emission declines as $\nu^{-(2+\beta)}$ where $\beta \sim 1$. Early submillimeter/millimeter polarimetry was done using at 850 μm with the single bolometer UKT 14 on the JCMT and at 1.3 mm with MILLIPOL on the NRAO 12m (Clemens et al. 1990).

Current instrumentation utilizes sensitive bolometer arrays to map relatively large areas with high sensitivity. The SCUBA polarimeter on the JCMT (Greaves et al. 2003) operates primarily at 850 μm, with a resolution of 14$''$. The Hertz polarimeter (Dowell et al. 1998) on the CSO operates at 350 μm with a resolution of 20$''$. Additionally, the BIMA array (Welch et al. 1996) has done substantial high resolution dust polarimetry at 1.3 mm.

The wealth of spectral lines observable in the submillimeter/millimeter regime provides an alternate means of probing the magnetic field geometry. Linear polarization of line emission as described by Goldreich & Kylafis (1981, 1982) has now been detected in several protostellar outflows and even in a star-forming core. Molecular spectroscopy also yields information about the inclination of the magnetic field by comparison of spectral lines from co-spatial ionic and neutral species (Houde et al. 2000a,b).

3. Magnetic Fields on Large Scales

On molecular cloud scales, observations of magnetic fields are particularly difficult. Simulations of MHD turbulence predict the development of filamentary structures similar to those seen inside molecular clouds (Heitsch et al. 2001).

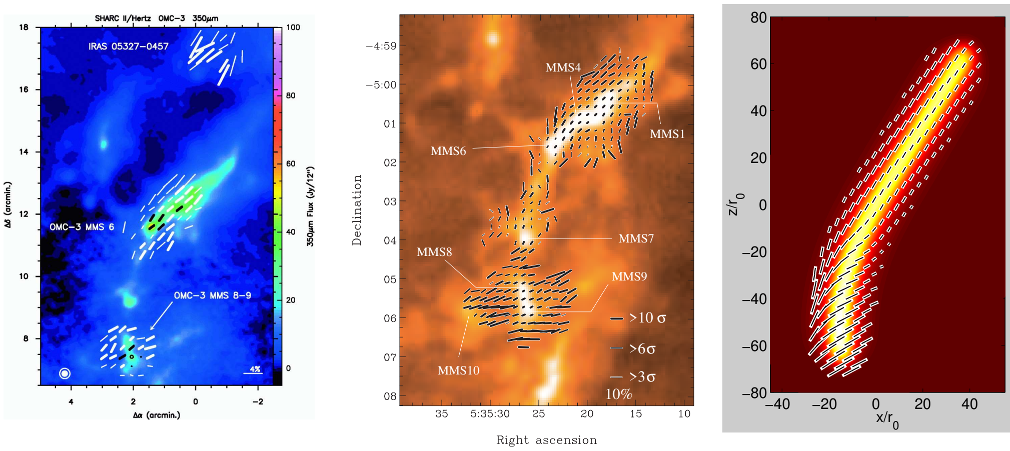

Figure 2. The OMC-3 region of the Orion A filament is shown in polarized 350 μm emission (left, Houde et al. 2004) and 850 μm emission (center; Matthews et al. 2001). Based on their data, Matthews et al. (2001) asserted that the field geometry in OMC-3 had to be complex, since no straight geometry could produce the polarization pattern observed. The helical field model of Fiege & Pudritz (2000a,b) produced a polarization pattern similar to the observations (right).

The best studied filamentary component of a molecular cloud is the integral shaped filament of Orion A. Figure 2 shows the polarization pattern observed at 850 μm and the analytic model of those data produced using a static helical field geometry (Matthews, Wilson & Fiege 2001). A more complete polarization map of the filament has been produced using the Hertz polarimeter on the CSO (Houde et al. 2004); these data show a similar polarization pattern in OMC-3 (see Figure 2), but with much more consistency between the MMS6 and MMS8-9 regions in polarization position angle.

These data and those of other filamentary clouds in Orion B (NGC 2024, see Figure 3 and NGC 2068, Matthews & Wilson 2002a) show that on the largest scales thus measurable in polarized emission, the polarization patterns can be very complex. Based on simulations of turbulence in molecular clouds (Heitsch et al. 2001; Ostriker, Stone & Gammie 2001; Padoan et al. 2001), straight fields should not be expected on large scales. Unfortunately, observations are not yet sensitive enough to map field geometries toward extended molecular material of $A_v \lesssim 10$. Therefore, only the brightest filamentary structures have been mapped with the current generation of chopping detectors.

4. Preservation of Field Geometry from Clouds to Cores

In order to determine whether the field geometry of star-forming cores is inherited unchanged from larger scale structures, observations are needed both of the lower density dust and the high density cores. Field geometries of compact protostellar cores are best determined using interferometers, since their characteristic spatial filtering means the instrument is sensitive only to spatial structures over a narrow range of scales[1], unlike single dishes which detect the total emission on all scales within the cloud. The single dish polarization data yield a density-weighted vector sum through the cloud, making them most sensitive to dense structures. However, in many clouds, this emission contains substantial contributions from the material in which cores are embedded. This dust is in an environment of $N(H_2) \approx 10^{23}$ cm^{-3}, corresponding to hundreds of magnitude of A_v. Based on observations (i.e., Vaillancourt 2002) and theory (i.e., Lazarian, Goodman & Myers 1997), these warmer grains are expected to produce more polarization than cold grains in cores.

Figure 3 contains the single dish polarimetry map of NGC 2024's filamentary ridge and the interferometric map of the brightest core, FIR5 (Lai et al. 2002). The BIMA array data of Lai et al. clearly show that a similar field geometry exists in the core as is detected on a scale 10× larger in the JCMT and KAO maps. However, the BIMA data cover a region of approximately 1-2 JCMT beams, so the variation in the BIMA data would cancel along the filament axis in the JCMT beam. The core's field geometry appears very ordered and does not represent a disarray of polarization position angles, as would be expected in a turbulence dominated core (e.g., Padoan et al. 2001), but it is noteworthy that cores with ordered magnetic field geometries can still be supported by turbulence (see § 6.2.).

[1]The spatial filtering of interferometers can also create difficulties in interpreting these data. Missing flux and spatial structure can be replaced by combinations of single dish and interferometric data. Unfortunately, the wavelengths of submillimeter single dish polarimeters and millimeter interferometers are mutually exclusive.

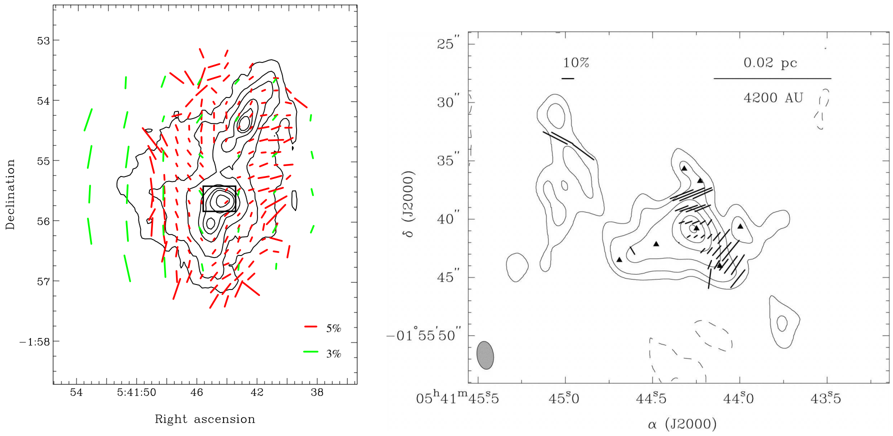

Figure 3. The filamentary ridge NGC 2024 in Orion B exhibits an ordered "V" shaped polarization pattern when observed with at 850 μm (black, Matthews, Fiege & Moriarty-Schieven 2002) and 100 μm (grey, Dotson et al. 2000). The box is the dimension of the BIMA map at right. Interestingly, the interferometric data of the FIR5 core mirrors this polarization pattern (Lai et al. 2002). The polarization vectors (with a resolution of 2″) on the core are not precisely straight, but exhibit an ordered curvature as discussed by Lai et al. (2002).

In contrast, Barnard 1, a dark cloud core in Perseus, contains several cores from which polarized emission has been detected (Matthews & Wilson 2002b). In this case, the polarization from the ambient material is also detected (see Figure 5). Each of the cores has an ordered field geometry indicated by the high degree of alignment in the vectors. However, the ambient dust exhibits a different orientation, implying that the core geometry is not inherited unaltered from the lower density material.

5. Polarization Holes

The presence of declining polarization with increasing flux has been observed almost universally in submillimeter and millimeter maps, regardless of the observing wavelength or resolution. The effect is not limited to cores alone, since the Orion A filament itself exhibits this effect in a region devoid of cores (Matthews et al. 2001). The explanations of this "depolarization" fall into two categories: magnetic field geometry (cancellation in a beam or systematic changes through the cloud) or poor grain alignment (due to changing grain physics or the absence of an aligning field). Figure 4 shows the single dish and interferometric polarization patterns of the massive core OMC-1. These two patterns are strikingly different, with the BIMA array data revealing small-scale 90° changes in polarization position angle. Rao et al. (1998) suggest that these changes could occur in OMC-1 owning to its high outflow activity which can act to align grains with their long axes parallel to the magnetic field (Gold 1952). Houde et al. (2004) note, however, that depolarization is observed elsewhere in the OMC-1 single dish map; it is not limited to the peak of the OMC-1 core.

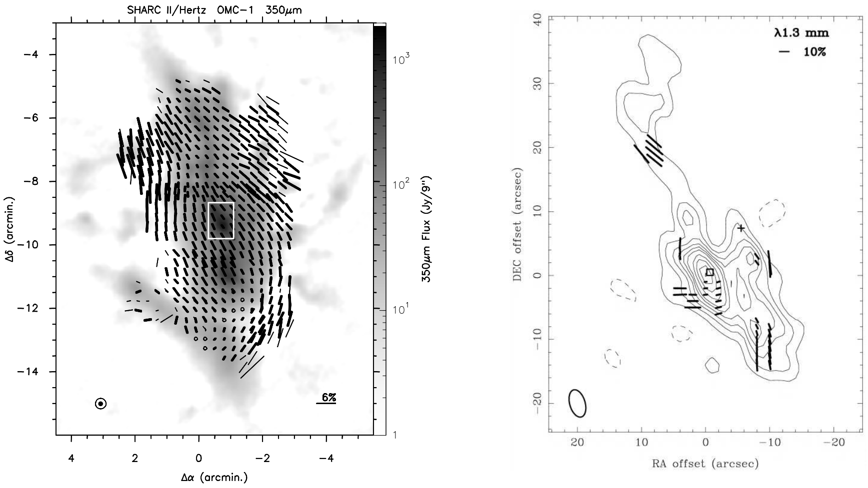

Figure 4. Polarization patterns in the OMC-1 core at 350 μm from the CSO (Houde et al. 2004) and at 1.3 mm from the BIMA array (Rao et al. 1998). The white box shows the region covered by the BIMA map. Improved resolution provides an explanation for the polarization hole observed in the single dish map since orthogonal vectors cancel within the larger beam.

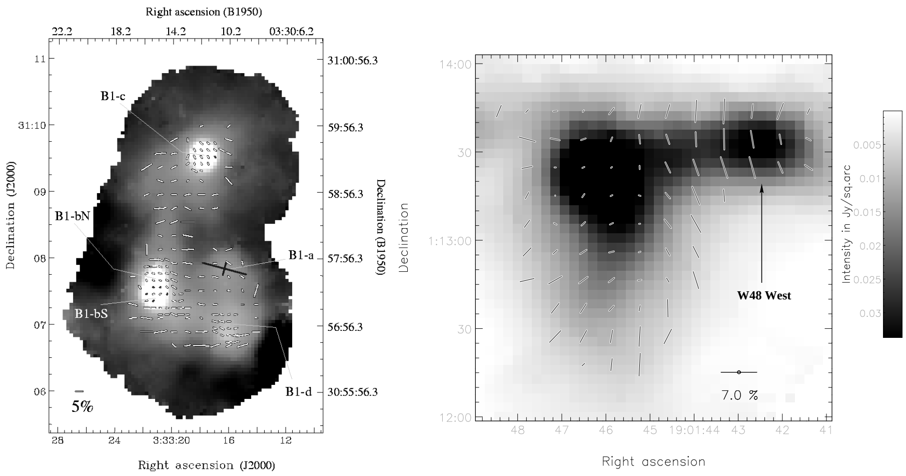

Figure 5. These two regions contain cores for which no appreciable depolarization has been detected toward the peaks. The B1-c core (left) in Perseus has a mass of about 6 $M_{\odot}$ (Matthews & Wilson 2002b); the W48 West core (right) has a mass of 1500 $M_{\odot}$ (Curran et al. 2004).

Recently, several datasets have emerged which do not exhibit polarization holes. The first was Core C in Barnard 1 (Matthews & Wilson 2002b). In a more recent survey of high mass protostellar objects and candidates, 2 of 20 cores observed did not exhibit significant depolarization (R. Curran, private communication). These cores, W48 West and S152SE, are candidate high mass protostellar objects (HMPOs) with age estimates consistent with the pre-stellar phase (Curran et al. 2004). Figure 5 shows the low mass core B1-c and the HMPO candidate W48 West. Their masses differ by a factor of 250. Each has formed in a very different region, but one distinguishing characteristic of them both is their extreme youth.

However, the presence of polarization holes is clearly not purely an evolutionary trait, however, since starless cores observed in Taurus and Ophiuchus do show diminished polarization percentage toward regions of higher flux (see L83 and L143 in Figure 1). Nor is the effect purely one of resolution as is the case for OMC-1; Figure 3 demonstrates that small scale magnetic field structure can mirror large scales. Furthermore, the HMPO candidates without polarization holes detected by Curran et al. (2004) both are adjacent to cores which do exhibit depolarization.

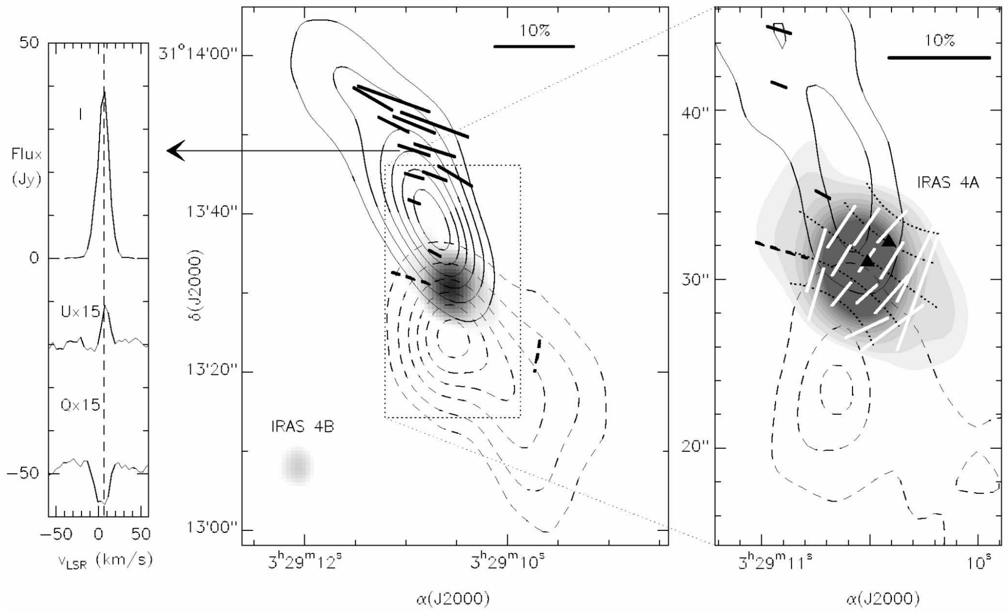

Figure 6. Dust and CO intensity (greyscale and contours) with polarization data (white and black respectively) toward the Class 0 protostar NGC1333 IRAS4A, observed with the BIMA array. The alignment of the CO polarization lies primarily along the outflow axis and perpendicular to the dust polarization direction. The outflow is nearly parallel to the axis of symmetry of the dust core near the protostar, but bends at larger distances. Girart et al. (1999) estimated that a 150 μG field would be sufficient to deflect the outflow by the action of the magnetic field. The dust polarization data are consistent with a so-called "hourglass" field geometry (dashed lines) which has also been noted in OMC-1.

6. Spectroscopy

6.1. Linear Polarization of Spectral Lines

Goldreich & Kylafis (1981, 1982); Kylafis (1983) describe the conditions under which linear polarization of spectral lines can occur. In star-forming regions, the Goldreich-Kylafis Effect has been observed in the Galactic center (Greaves et al. 1999), the outflow of FIR5 in NGC 2024 (Greaves, Holland & Ward-Thompson 2001) and the DR21(OH) core MM1 (Lai, Girart & Crutcher 2003b). The first interferometric detection was in the outflow of the Class 0 protostar NGC 1333 IRAS4A (Girart, Crutcher & Rao 1999), as shown in Figure 6.

Depending on the physical conditions, the polarization generated from spectral lines may be either parallel or perpendicular to the local magnetic field. In Figure 6, the polarized CO is aligned orthogonally to the dust polarimetry, which is expected to align perpendicular to the magnetic field (Hildebrand 1988). Hence, based in the dust polarimetry toward the core, Girart et al. (1999) interpreted the magnetic field as aligning along the outflow axis, parallel to the detected polarization direction.

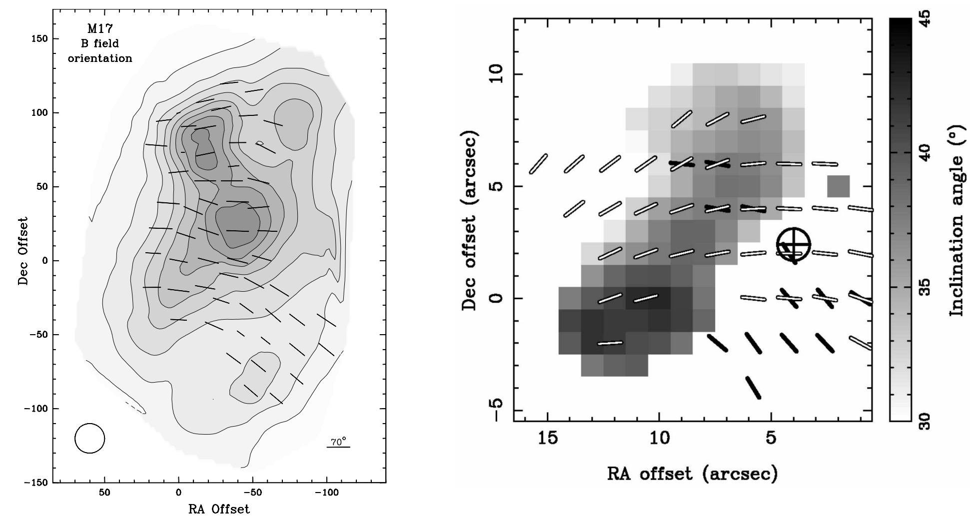

Figure 7. Determination of the orientation of the magnetic field in the M17 molecular cloud (left, Houde et al. 2002). The projected direction of the field on the plane of the sky is shown by the vector direction and the viewing angle of the total field vector to the line of sight is shown by the vector length. The magnetic field structure of MM1 (right, Lai et al. 2003a). The greyscale shows the inclination of the magnetic field to the line of sight; the vectors illustrate the plane-of-sky field orientation inferred from dust (black) and CO (white) polarized emission. The encircled plus sign represents the position of the CN Zeeman measurement of the line-of-sight field component.

6.2. Comparisons of Ionic and Neutral Spectra

In a series of papers, Houde et al. (2000a,b) have demonstrated a method for determination of the inclination of the magnetic field to the line of sight which, where applicable, could maximize the information about the total three-dimensional magnetic field in regions where either the linearly polarized dust or spectral line data or Zeeman splitting observations can produce a field estimate. These techniques are not generally sensitive to magnetic fields in identical physical environments because dust polarimetry is most successful at densities exceeding the critical density of OH ($\sim 10^4$ cm^{-3}), the most commonly utilized molecule for Zeeman splitting observations. Figure 7 shows the results of this technique in the molecular cloud M17 (Houde et al. 2002) and within the MM1 core of DR21(OH), hereafter just called "MM1" (Lai, Velusamy & Langer 2003a).

7. Turbulence or Magnetic Fields?

The alignment of vectors detected in the cores of Barnard 1 imply that the field is highly ordered. In addition, the absence of a polarization hole in B1c suggests that grains are aligned at high densities within the core. Observations of N_2H^+ 1–0 emission from the core reveal non-thermal linewidths. The Chandrasekhar-Fermi (CF) Method (Chandrasekhar & Fermi 1953) utilizes the dispersion of the polarization vectors to yield a lower limit to the field strength of 380 μG, taking into account the factor of 0.5 needed to compensate statistically for overestimation of the field strength (Heitsch et al. 2001; Ostriker et al. 2001). This field strength greatly exceeds the line-of-sight field strength of -27μG measured directly from Zeeman splitting measurement of OH (Goodman et al. 1989) in a $2.9'$ beam. A comparison of the energy densities for reasonable estimates of density (2×10^6 cm^{-3}) and radius (10^4 AU) produces comparable values for turbulent and magnetic energies, where the magnetic energy is a lower limit since the polarimetry probes only two of the three field dimensions. Both the magnetic and turbulent energies exceed the gravitational energy; hence, this core appears sub-critical with sufficient magnetic support to prevent collapse.

In MM1, both dust and CO polarimetry as well as a Zeeman splitting detection of the line-of-sight field strength exist. Therefore, Lai et al. (2003b) were able to compare the field strength derived from the CF method to the estimate produced from the line-of-sight strength once the inclination of the field to the line of sight was measured. Using CN, Crutcher et al. (1999) estimate $B_{los} \sim -0.36$ mG. The comparison of neutral to ionic spectra suggests that the field inclination is quite uniform across the MM1 core, with an inclination to the line of sight of 36° (Lai et al. 2003a). These data imply a plane-of-sky field strength of 0.25 ± 0.07 mG and a total field strength of 0.44 ± 0.12 mG. Using the CF method applied to the dispersion of the CO polarization position angles, Lai et al. (2003b) found $B_p = 0.9$ mG, substantially larger than that derived from the Zeeman measurement of B_{los} and the field incliation. Based on the total field strength of 0.44 mG and the spectroscopy in the core, MMS1 is found to be magnetically supercritical but dominated by turbulent, not magnetic, support. Hence, evidence of an ordered field geometry does not necessarily imply that turbulence is neither present nor significant.

8. Summary

The present generation of single dish and interferometric polarimeters have vastly broadened our observational picture of the complexities of the magnetic field in star-forming regions. The advantages of sensitive bolometric arrays in mapping the more extended structures from which cores form are evident. Some complex polarization patterns are revealed which suggest field geometries are ordered on large scales (i.e., on the order of a parsec). Polarized dust emission is detected on all scales and at all wavelengths observed in molecular clouds (to sensitivity limits).

Polarization holes continue to be detected toward many regions of varying age, distance and mass. Where high resolution data are available, the data suggest that cancellation of polarization vectors in the beam (arising either from changes in field geometry or alignment mechanisms) could be the cause. However, it is noteworthy that even the interferometric data demonstrate depolarization toward the high intensity peaks. Hence, if variation in vector orientation is truly the source of the polarization holes, then the variation must be occurring on scales $<$ 1000 AU in cores (using FIR5 of Figure 3 as an example). Of equal interest are the cores detected without depolarization. Comparison of their properties with those of cores with polarization holes could yield real insight into the conditions giving rise to the changes in polarization percentage we observe.

The most innovative new observational technique is the use of spectral line data of neutral and ionic species to measure the inclination of the magnetic field to the line of sight. Particularly where Zeeman splitting observations are successful, this method can yield a solid total field stength without appealing to statistical averages. The CF method of using the dispersion of polarization vectors to estimate the field seems to systematically overestimate the field strength. The data of MM1 illustrate how large the overestimation can be even with the statistical correction derived from numerical simulations.

The future looks bright for continued development of this area of star formation studies. On single dishes, the next decade will see more powerful polarimeters installed at many more wavelengths than are currently accessible. These include the 350 μm Hertz-II polarimeter at the CSO, the 850/450 μm SCUBA-2 and 345 GHz heterodyne ROVER polarimeters on the JCMT, the 870 μm PolKa (ultimately for use on APEX, Siringo et al. 2004), and the 50-200 μm Hale polarimeter on SOFIA. Three interferometers also will provide important polarimetry maps of star forming cores: the SubMillimeter Array (especially at 345 GHz), the Combined Array for Research in Millimeter-Wave Astronomy (115 and 230 GHz) and the Atacama Large Millimeter Array (potentially 230 - 660 GHz). ALMA in particular will have the sensitivity and resolution to investigate the magnetic field in protostellar disks and outflows to the extent that tests of collimation models should be possible. One expects that the improved sensitivity and wavelength accessibility of the next generation of interferometers will accomplish for our understanding of magnetic fields on small scales what sensitive bolometric arrays have done for their study on larger scales.

One use of polarized dust emission which I have not discussed is the comparison of data at different wavelengths (the polarization spectrum) to constrain the properties of dust grain populations as discussed by Hildebrand et al. (1999) and applied to OMC-1 by Vaillancourt (2002). For most regions, polarimetry exists at only a few wavelengths or is obtained with instruments which probe different dust populations (e.g., single dish telescopes versus interferometers). Single dish telescopes operating at the same wavelengths as interferometers could permit a high resolution analysis of dust grain properties, if data from the two instruments is combined to produce a total power polarization map.

The most effective instrument for spectropolarimetry has been the BIMA array, which was shut down in June 2004 for the move to CARMA. This is partly due to the strength of the CO line in the interferometric beam, but also because the Goldreich-Kylafis Effect is stronger for lower excitation lines. Therefore, even though the CO $3-2$ emission is very strong, the single beam heterodyne polarimetry on the JCMT has thus far limited the usefulness of this technique. The new 1.3 mm XPOL polarimeter built for the IRAM 30m is designed for both continuum and heterodyne work. In addition, the new ROVER polarimeter on the JCMT will accompany the heterodyne array HARP, making polarimetry mapping of spectral lines at 345 GHz feasible.

On the largest scales in molecular clouds, the major limitation to polarimetric mapping is technique of chopping at several Hz to remove the sky noise which dominates submillimeter observing. The JCMT has a maximum chop throw of $3'$, while the CSO can reach $6'$. In regions of low A_v in molecular clouds, emission is typically smooth enough that chopping effectively cancels all signal. This limitation remains the largest observational constraint to testing numerical simulations of MHD turbulence in clouds and understanding how the magnetic field of molecular clouds maps onto those of the more diffuse warm neutral medium.

References

Bourke, T.L., Myers, P.C., Robinson, G., & Hyland, A.R. 2001, ApJ, 554, 916
Chandrashekar & Fermi 1953, ApJ, 118, 113
Clemens, D.P., Kane, B.D., Leach, R.W., & Barvainis, R. 1990, PASP, 102, 1064
Crutcher, R.M. 1999, ApJ, 520, 706
Crutcher, R., Nutter, D., Ward-Thompson, D. & Kirk, J. 2004, ApJ, 600, 279
Crutcher, R.M., Troland, T.H., Lazareff, B., Paubert, G. & Kazès, I. 1999, ApJ, 514, L121
Curran, R.L., Chrysostomou, A., Collett, J.L., Jenness, T., & Aitken, D.K. 2004, A&A, 421, 195
Dotson, J.L., Davidson, J., Dowell, C.D., Schleuning, D.A., & Hildebrand, R.H. 2000, ApJS, 128, 335
Dowell, C.D., Hildebrand, R.H., Schleuning, D.A., Vaillancourt, J.E., Dotson, J.L., Novak, G., Renbarger, T., & Houde, M. 1998, ApJ, 504, 588
Elmegreen, B.G. 2000, ApJ, 530, 227
Fiege, J.D. & Pudritz, R.E. 2000, MNRAS, 311, 85
Fiege, J.D. & Pudritz, R.E. 2000, ApJ, 544, 830
Girart, J.M., Crutcher, R.M., & Rao, R. 1999, ApJ, 525, L109
Gold, T. 1952, MNRAS, 112, 215
Goldreich, P., & Kylafis, N.D. 1981, ApJ, 243, L75
Goldreich, P., & Kylafis, N.D. 1982, ApJ, 253, 606
Goodman, A.A., Crutcher, R.M., Heiles, C., Myers, P.C., & Troland, T.H. 1989, ApJ, 338, L61
Greaves, J.S., et al. 2003, MNRAS, 340, 353

Greaves, J.S., Holland, W.S., & Ward-Thompson, D. 2001, ApJ, 546, L53
Greaves, J.S., Holland, W.S., Friberg, P., & Dent, W.R.F. 1999, ApJ, 512, L139
Hartmann, L., Ballesteros-Paredes, J. & Bergin, E.A. 2001, ApJ, 562, 852
Heitsch, F., Zweibel, E.G., Mac Low, M.-M., Li, P., & Norman, M.L. 2001, ApJ, 561, 800
Hildebrand, R.H. 1988, QJRAS, 29, 327
Hildebrand, R.H., Dotson, J.L., Dowell, C.D., Schleuning, D.A., & Vaillancourt, J.E. 1999, ApJ, 516, 834
Houde, M., Dowell, C.D., Hildebrand, R.H., Dotson, J.L., Vaillancourt, J.E., Phillips, T.G., Peng, R., & Bastien, P. 2004, ApJ, 604, 717
Houde, M., Phillips, T.G., Bastien, P., Peng, R., & Yoshida, H. 2002, ApJ, 569, 803
Houde, M., Peng, R., Phillips, T.G., Bastien, P., & Yoshida, H. 2000b, ApJ, 537, 245
Houde, M., Bastien, P., Peng, R., Phillips, T.G., & Yoshida, H. 2000a, ApJ, 536, 857
Kylafis, N.D. 1983, ApJ, 267, 137
Lai, S.-P., Crutcher, R.M., Girart, J.M., Rao, R. 2001, ApJ, 561, 864
Lai, S.-P., Crutcher, R.M., Girart, J.M., Rao, R. 2002, ApJ, 566, 925
Lai, S.-P., Girart, J.M., & Crutcher, R.M. 2003b, ApJ, 598, 392
Lai, S.-P., Velusamy, T., & Langer, W.D. 2003a, ApJ, 596, L239
Larson, R.B. 1981, MNRAS, 194, 809
Lazarian, A., Goodman, A.A., & Myers, P.C. 1997, ApJ, 490, 273
Levin, S.M., Langer, W.D., Velusamy, T., Kuiper, T.B.H., & Crutcher, R.M. 2001, ApJ, 555, 850
Matthews, B.C., Fiege, J.D., & Moriarty-Schieven, G.H. 2002, ApJ, 569, 304
Matthews, B.C., & Wilson, C.D. 2002a, ApJ, 574, 822
Matthews, B.C., & Wilson, C.D. 2002b, ApJ, 571, 356
Matthews, B.C., Wilson, C.D., & Fiege, J.D. 2001, ApJ, 562, 400
Ostriker, E.C., Stone, J.M., & Gammie, C.F. 2001, ApJ, 546, 980
Padoan, P., Goodman, A.A., Draine, B., Juvela, M., Nordlund, Å., & Rögnvaldsson, Ö. 2001, ApJ, 559, 1005
Rao, R., Crutcher, R.M., Plambeck, R.L., & Wright, M.C.H. 1998, ApJ, 502, L75
Siringo, G.P., Kreysa, E., Reichertz, L.A., & Menten, K.M. 2004, this volume
Vaillancourt, J.E. 2002, ApJS, 142, 53
Vázquez-Semadeni, E., Ballesteros-Paredes, J. & Klessen, R. 2003, ApJ, 585, 131
Ward-Thompson, D., Kirk, J.M., Crutcher, R.M., Greaves, J.S., Holland, W.S., & André, P. 2000, ApJ, 537, L135
Welch, W.J. et al. 1996, PASP, 108, 93